

## Charge Inversion by Flexible Polyelectrolytes Adsorbed onto Charged Cylindric Surfaces within Self-Consistent-Field Theory

Xingkun Man and Dadong Yan\*

*Beijing National Laboratory for Molecular Sciences (BNLMS), Institute of Chemistry, Chinese Academy of Sciences, Beijing 100190, China*

*Received October 7, 2009; Revised Manuscript Received January 29, 2010*

**ABSTRACT:** Self-consistent-field theory (SCFT) is presented to study the charge inversion phenomena by flexible polyelectrolytes (PE) adsorbed onto oppositely charged cylindric surfaces. We focus on the effect of surface curvature on the charge inversion ratio between the area density of surface charge compensated by the adsorbed polymers and the area density of origin surface charge. Numerical results show that surface curvature does have a strong effect on the charge inversion phenomena. Namely, it can lead to strong charge inversion at high salt concentrations with strong surface–PE short-range non-Coulombic interaction even in a good solvent. In particular, under large surface curvature and strong short-range non-Coulombic interaction conditions, full charge inversion can even happen at low salt concentrations. Moreover, numerical results show that the surface curvature has a different effect on the charge inversion ratio in the regime dominated by the surface–PE electrostatic interaction and in the regime dominated by the surface–PE short-range non-Coulombic interaction. Increasing surface curvature will decrease the charge inversion ratio in the former case, while it will increase it in the latter case. Also, we numerically obtain a crossover point for the cylinder radius, which approximately equates to 2 times the gyration radius of PE chain. When the cylinder radius becomes larger than it, the surface curvature will lose its effect on the charge inversion. The numerical results give a further demonstration that, in these weakly charged systems, the surface–PE short-range non-Coulombic interaction is the main driving force of charge inversion phenomena. The results are in good agreement with the theoretical and experimental results.

### I. Introduction

Polyelectrolytes (PE) adsorbed onto oppositely charged surfaces have generated a great deal of attention in recent years due to their numerous biological and industrial applications.<sup>1–5</sup> Although a full description of PE adsorption is still lacking at present, some general conclusions of the PE adsorption mechanism exist; for example, the factors which can govern the properties of the PE adsorption are agreed to be the charge fraction of each PE chain,  $p$ , the density of surface charge,  $\sigma$ , the salt concentration,  $C_{\text{salt}}$ , the solvent quality, and the surface geometry. Meanwhile, the essential effects of these factors on the PE adsorption are reflected via their direct effect on the three interactions existing in PE adsorption systems, i.e., the surface–PE electrostatic interaction, the surface–PE short-range non-Coulombic interaction, and the entropy consideration, and all three can control the PE adsorption.

By increasing the charge fraction of PE chain, it can lead to both an increase and a decrease of PE adsorption. The reason is that increasing the value of  $p$  from 0 first can enhance the surface–PE electrostatic interaction and results in the increase of PE adsorption. However, when  $p$  is large enough, the monomer–monomer repulsion begins to hinder the adsorption of PE. Meanwhile, the salt concentration has a similar role as  $p$ . The reason is that it can screen both of the monomer–monomer repulsion and the surface–PE electrostatic interaction, which can result in different effects on the PE adsorption. The solvent quality is mainly responsible for the surface–PE short-range non-Coulombic interaction because strongly hydrophobic PE–backbone can increase this interaction and results in

adsorbing more PE onto the surface. Moreover, the different surface geometry can lead to different entropy penalty of PE chains after being adsorbed onto surfaces. These three interactions always coexist in PE adsorption systems, and the interplay among them gives diverse interesting phenomena.

Charge inversion is just one of the most interesting phenomena. Namely, when the charges of the adsorbed PE chains overcompensate the original surface charges, the surface–PE complex will have charges opposite to that of the bare charged surface. This phenomenon has been observed in experiments<sup>6–8</sup> and plays an essential role in the buildup of PE multilayers via the electrostatic layer-by-layer assembly onto an adsorption surface.<sup>9–11</sup> Thousands of experimental works related to this topics have been done. These results show that the main factors, which can control the structure of such electrostatically bound multilayers, are pH value<sup>7,12,13</sup> and salt concentration.<sup>14,15</sup> It was found that by varying the pH value the surface charge, the PE backbone charge, and the layer thickness can be altered dramatically. Specially, large overcompensation of the substrate charge caused by PE for low pH values has been established.<sup>7</sup> The pH value can also control the stability of the PE multilayers.<sup>13</sup> Meanwhile, as salt can screen the electrostatic interaction between all charges, it has pronounced effects on the layer thickness. These studies<sup>6–15</sup> show that the surface–PE electrostatic interaction is the main driving force in the growth of PE multilayers.

In the past 10 years, however, more and more results from both experimental and theoretical studies have shown that the surface–PE short-range non-Coulombic interaction also plays an important role in the growth and the stability of PE multilayers. Such interactions, also called chemical interaction,<sup>16,17</sup> include hydrophobic interaction,<sup>18,19</sup> hydrogen bonding,<sup>13,20,21</sup> and other water structure-mediated interactions.<sup>16</sup> Kotov<sup>18</sup> first brought in

\*Corresponding author. E-mail: yandd@iccas.ac.cn.

the hydrophobic interaction in layer-by-layer adsorption, while Stockton and Rubner<sup>20</sup> showed the first demonstration of hydrogen bonding as the basis for alternating polyion assembly. The typical theoretical works on the buildup of PE multilayers were carried out by Shafir, Andelman,<sup>16,22</sup> and Wang.<sup>23,24</sup> They solved the relevant mean-field equations numerically with special boundary conditions to study the adsorption of flexible PE onto oppositely charged planar surfaces. Their numerical results show that the full inversion of surface charge caused by adsorbed PE occurs only for the high salt concentration and strong surface–PE short-range non-Coulombic interaction. In particular, they found that no charge inversion happened for chemical nonadsorbing surfaces.

However, the surface curvature has been less studied, which can also affect the properties of PE multilayers. In a related work,<sup>25</sup> we demonstrated that the surface curvature does have an effect on the criteria of PE adsorption. Other theoretical and experimental studies also show the effect of surface curvature on the PE adsorption. Muthukumar et al.<sup>26,27</sup> used a combination of variational calculation and the ground state dominance to study the PE adsorption onto charged planar, cylindric, and spherical surfaces, in which they obtained different critical criteria of PE adsorption. Winkler and Cherstvy<sup>28</sup> analytically investigated the critical adsorption of a PE chain onto a spherical surface by substituting the Hulthén potential for the Debye–Hückel potential. Their results give a different scaling law of critical quantities from the planar case. Dubin et al.<sup>29,30</sup> experimentally showed that the surface curvature does have effects on the criteria of PE adsorption. Furthermore, Netz et al.,<sup>31–34</sup> Gurovitch et al.,<sup>35</sup> and Golestanian<sup>36</sup> studied the adsorption of one polyelectrolyte chain on oppositely charged curvature surfaces. With the assumption that there are only electrostatic interactions between the surface and PE chain, they showed that when the curvature of the small colloidal particles is large enough, it can lead to a much more pronounced effect for PE adsorption as compared with neutral polymer. However, there are few works directly investigate the effects of surface curvature on the charge inversion phenomena in multichain systems up to present. Therefore, we extend the continuum self-consistent-field theory (SCFT) of inhomogeneous multicomponent polyelectrolytes systems, which is developed by Shi<sup>37</sup> and Wang,<sup>38</sup> to directly study the effect of surface curvature on the charge inversion phenomena in cylindric systems. The motivation to study this phenomena is due to the fact that many biomacromolecules have rodlike appearances<sup>3</sup> such as the tobacco mosaic virus (TMV)<sup>39</sup> and the heparin–peptide amphiphile complex.<sup>40</sup>

In this paper, we use the continuum SCFT to study the charge inversion phenomena which is caused by adsorbing flexible PEs onto oppositely charged cylindric surfaces. According to previous work,<sup>16,41</sup> PE adsorption has different behaviors in the surface–PE electrostatic interaction dominated regime and short-range non-Coulombic interaction dominated regime. Naturally, we mainly focus on the effect of surface curvature on the charge inversion phenomena in these two regimes. Theoretical model and numerical method are presented in section II. Results and discussions are presented in section III. Conclusions are summarized in section IV.

## II. Theoretical Framework

In this paper, we consider a solution which contains a positively charged cylinder with area density of surface charges,  $\sigma_0$ , in the center of the system, a bulk concentration of flexible negatively charged homopolymers,  $\phi_{p,b}$ , with fixed charge fraction,  $p$ , a bulk concentration of salt ions,  $C_{s,b}$ , and counterions from the cylinder and PEs. As we assume that the system has a cylindric symmetry, the calculation can be done only in one dimension

along the radial direction of the cylinder. The center of the cylinder is taken at  $r = 0$ , and the distance from the cylinder surface to the boundary of the bulk phase is  $L$ . In all the calculations, we take a large enough value of  $L$  to make sure that we can treat the boundary part as a reservoir or a bulk solution. After many attempts, we find that  $L > 50R_g$  looks suitable for the calculation, where  $R_g$  is the gyration radius in bulk PE. Since  $L$  is large enough, we can use a canonical ensemble to treat such a grand canonical system. Throughout this paper we assume, for simplicity, that the polyion and the small ions are all monovalent. Here the small ions come from PE chains, charged surface counterions, and dissolved salt. Also, we assume that all the small ions are identical and denoted by  $\pm$  for cations and anions, respectively.

Besides the electrostatic interactions between charges, we add a short-range non-Coulombic interaction between the cylindric surface and the polymer monomers to the Hamiltonian of the system. The way to deal with such an interaction follows the previous work,<sup>42</sup> in which the surface–PE short-range non-Coulombic interaction,  $U(r)$ , extends over distance on the order of the Kuhn length,  $a$ , and has a rectangular-form potential for simplicity. In the cylindric coordinates, it is assumed to have the form as follows:

$$U(r) = \begin{cases} 0 & r > r_0 + d \\ U_0 & r_0 \leq r \leq r_0 + d \end{cases}$$

Here,  $r_0$  is the cylinder radius and  $U_0$  is a constant in units of  $k_B T$ , where  $k_B$  is the Boltzmann constant and  $T$  is the temperature;  $d$  is the range of adsorption and of the order of  $a$ , i.e.,  $d = 2a \approx R_g/3$ , where  $a$  is the Kuhn length. Therefore, within SCFT the free energy functional of such ionic solution is given by<sup>25,37</sup>

$$\begin{aligned} \frac{\mathcal{F}[\phi, \varphi]}{\rho_0} = & \int d^3r \left[ \sum_j \mu_j \phi_j(r) + \chi_{Ps} \phi_P(r) \phi_s(r) \right] \\ & - \int d^3r \left[ \sum_j \omega_j(r) \phi_j(r) + e \omega_e(r) \phi_e(r) \right] - \sum_j \frac{\bar{\phi}_j V}{Z_j} \ln \left( \frac{Q_j}{\bar{\phi}_j} \right) \\ & + \int d^3r \left[ \phi_e(r) \varphi(r) - \frac{a^2}{2\tau} |\nabla \varphi(r)|^2 \right] + \int d^3r \phi_P(r) U(r) \quad (1) \end{aligned}$$

where  $\varphi(r)$  is the electrostatic potential and normalized by  $k_B T/e$  to make it dimensionless ( $e$  is the unit charge);  $\rho_0$  is a reference monomer density;  $\phi_j(r)$  is the dimensionless volume fractions of PE monomer, solvent, and small ions with  $j = P, s, \pm$ , respectively;  $\omega_j(r)$  are the auxiliary fields which couples with the volume fractions  $\phi_j(r)$ , while  $\omega_e(r)$  is the auxiliary field for the charge density  $\phi_e(r) = -p\phi_P(r) + \phi_+(r) - \phi_-(r)$ ;  $Z_j$  is the degree of polymerization, i.e.,  $Z_P = N$  and  $Z_s = Z_{\pm} = 1$ ;  $Q_j$  are the single molecular partition functions. The definitions of  $\mu_j$ ,  $\chi_{Ps}$ , and  $\tau$  are the same as those in ref 37. Also, we take the same values for the parameters as our previous work,<sup>25</sup> such as the average Kuhn length  $a = 0.5$  nm, the Bjerrum length  $l_B = e^2/\epsilon k_B T \approx 0.7$  nm, and  $\tau^{-1} = 0.057$ .

Using the saddle-point approximation, additional to the incompressibility condition

$$\phi_P(r) + \phi_s(r) = 1 \quad (2)$$

we can obtain a set of self-consistent equations of densities, auxiliary fields, and electrostatic potential. Here, we ignore the volume of the small ions. The key quantity corresponds to the numerical solving these self-consistent equations is the

propagator,  $q(r, t)$ , the probability of finding the end monomer of a polyelectrolyte of length  $t$  at  $r$ , which can be obtained by solving the modified diffusion equation

$$\frac{\partial q(r, t)}{\partial t} = \frac{1}{6r} \frac{d}{dr} \left[ r \frac{dq(r, t)}{dr} \right] - [\omega_P(r) + p\varphi(r)]q(r, t) \quad (3)$$

with the initial condition  $q(r, t = 0) = 1$ , where  $t \in [0, N]$  is a variable along the chain contour. The boundary conditions for this diffusion equation are  $q(r = r_0, t) = 0$  and  $dq/dr|_{r=L} = 0$ .

The dimensionless volume fractions  $\phi_j(r)$  are given by

$$\begin{aligned} \phi_P(r) &= \frac{\bar{\phi}_P}{Q_P N} \int_0^N dt q(r, t) q(r, N-t) \\ \phi_s(r) &= \frac{\bar{\phi}_s}{Q_s} \exp[-\omega_s(r)] \\ \phi_{\pm}(r) &= \frac{\bar{\phi}_{\pm}}{Q_{\pm}} \exp[\mp\varphi(r)] \end{aligned} \quad (4)$$

where the average volume fractions are  $\bar{\phi}_j \equiv (1/L) \int_{r_0}^L dr \phi_j(r) = n_j Z_j / \rho_0 V$ , in which  $n_P$ ,  $n_s$ , and  $n_{\pm}$  are the total molecule numbers of PE chains, solvent molecules, cations and anions, respectively;  $V$  is the volume of the system. The single molecular partition functions,  $Q_j$ , are defined by

$$\begin{aligned} Q_P &= \frac{1}{L} \int_{r_0}^L dr q(r, N) \\ Q_s &= \frac{1}{L} \int_{r_0}^L dr \exp[-\omega_s(r)] \\ Q_{\pm} &= \frac{1}{L} \int_{r_0}^L dr \exp[\mp\varphi(r)] \end{aligned} \quad (5)$$

The auxiliary field  $\omega_s(r)$  can be obtained by a given sequence values of  $\omega_P(r)$

$$\omega_s(r) = \omega_P(r) + \chi[2\phi_P(r) - 1] - U(r) \quad (6)$$

Finally, the electrostatic potential  $\varphi(r)$  can be obtained by solving the Poisson–Boltzmann equation

$$\begin{aligned} &\frac{1}{r} \frac{d}{dr} \left[ r \frac{d\varphi(r)}{dr} \right] \\ &= -\tau \left\{ -p\phi_P(r) + \frac{\bar{\phi}_+}{Q_+} \exp[-\varphi(r)] - \frac{\bar{\phi}_-}{Q_-} \exp[\varphi(r)] \right\} \end{aligned} \quad (7)$$

we assume that  $\varphi(r) = 0$  in the bulk solution. In other words, the system locally charges neutrality in the bulk solution. With such a convention, we can rewrite eq 7 in the following form:

$$\begin{aligned} \frac{1}{r} \frac{d}{dr} \left[ r \frac{d\varphi(r)}{dr} \right] &= -\tau \{ -p\phi_P(r) + (C_{s,b} + p\phi_{P,b}) \exp[-\varphi(r)] \\ &\quad - C_{s,b} \exp[\varphi(r)] \} \end{aligned} \quad (8)$$

The boundary conditions of the Poisson–Boltzmann equation are  $d\varphi/dr|_{r=r_0} = -4\pi\sigma_B/a^2$  and  $d\varphi/dr|_{r=L} = 0$ , which correspond to a constant area density of surface charge. The dimensionless area density of surface charge is given by  $\sigma \equiv \sigma_0/a^{-2}$ , in which  $\sigma_0$  is the area density of surface charges (in unit charge  $e$ ).

We use the same numerical method as that in our previous work<sup>25</sup> to solve these self-consistent equations, which is based on the combination of Broyden's method and a globally convergent

strategy.<sup>43</sup> In all the calculations, we take care of the numerical mesh to make sure that it always less than the minimum value of the radius; e.g., all the numerical resolutions are less than 0.2. The main quantities which we focus on are the surface excess,  $\Gamma$ , and the charge inversion ratio,  $\sigma_{cp}/\sigma$ .  $\Gamma$  is defined as the total amount of PE monomers in the adsorption layer per unit length on the cylinder

$$\Gamma = \int_{r_0}^L dr r [\phi_P(r) - \phi_{P,b}] \quad (9)$$

$\sigma_{cp}$  is the effective area surface charge density compensated by the adsorbed polymers, given by  $\sigma_{cp} = \sigma - p\Gamma/r_0$ . Thus, the charge inversion ratio is given by

$$\sigma_{cp}/\sigma = 1 - p\Gamma/\sigma r_0 \quad (10)$$

Charge inversion only happens for  $\sigma_{cp}/\sigma < 0$ , and the full charge inversion will be observed when  $\sigma_{cp}/\sigma \leq -1$ . On the other hand,  $\sigma_{cp}/\sigma > 0$  means that no charge inversion happens. It is worth to note that the more negative value of  $\sigma_{cp}/\sigma$  corresponds to the larger charge inversion ratio.

We model separately two types of surfaces in this paper. One is nonadsorbing surface, while the other is chemically attractive surface. For the first kind of surface, there is only electrostatic interaction between the surface and PE monomers. However, for the second kind of surface, besides the electrostatic interaction, there is also a short-range non-Coulombic interaction between the surface and PE monomers. For the case without the surface–PE short-range non-Coulombic interaction results that the PE adsorption is mainly dominated by the electrostatic interaction, we call such regime as the electrostatic interaction dominated regime. It is easy to obtain such a regime by setting  $U_0 = 0$  in a salt-free solution. On the other hand, for the chemically attractive surface, the surface–PE short-range non-Coulombic interaction will enhance the surface adsorption ability. When this interaction becomes large enough to dominate the PE adsorption, the electrostatic interaction will have few effects on this adsorption process. We call such a regime as the short-range non-Coulombic interaction dominated regime. Whether the short-range non-Coulombic interaction dominates or not can be determined from the effects of salt concentration on the surface excess. Namely, the surface excess increases with increasing salt concentration in the short-range interaction dominated regime, while it decreases in the electrostatic interaction dominated regime.<sup>7,16,23,41</sup> In the present study, these two regimes can be determined by varying  $U_0$ . Experimentally, the Gibbs free energy, which is needed to compensate for the entropy loss of a monomer adsorbed onto a surface, is 0.2–0.4  $k_B T$ .<sup>17</sup> So we take the value of  $U_0$  from  $-0.5 k_B T$  to  $0 k_B T$  to make sure that we can obtain both of these two cases. We will investigate the effects of surface curvature on the PE charge inversion phenomena in both of the two regimes.

### III. Results and Discussion

Throughout this paper, the degree of polymerization of PE chains is  $N = 200$ , and hence the gyration radius is  $R_g = 5.8a$ . In the follows, all lengths are scaled by Kuhn length,  $a$ , and all the quantities with the dimension of energy are scaled by  $k_B T$ . All quantities including those in figures are represented in the scaled way. For  $a = 0.5$  nm and  $\rho_0 = a^{-3}$ , all the dimensionless volume fraction corresponds to real values multiplied by a factor  $\rho_0/N_A = 13.28$  mol/L, where  $N_A$  is Avogadro's number. According to these conventions,  $\phi_{P,b} = 1.25 \times 10^{-4}$  corresponds to the bulk molar density of polymer monomer  $\rho_P = 1.66$  mM, and  $C_{salt} = 0.1$  corresponds to the bulk molar concentration of

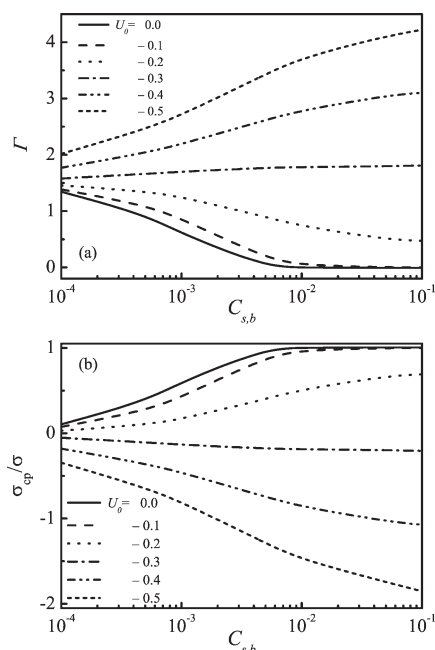


**Figure 1.** Effect of salt concentration on (a) surface excess,  $\Gamma$ , and (b) charge inversion ratio,  $\sigma_{cp}/\sigma$ , for several values of the short-range non-Coulombic interaction strength,  $U_0$ , with surface area charge density  $\sigma = 0.025$ , PE chain charge fraction  $p = 0.1$ , solvent quality  $\chi_{ps} = 0.1$ , and cylindrical radius  $r_0 = 6$ . The crossover is around  $U_0 = -0.3$ , at which both the surface excess and the charge inversion ratio nearly do not change with salt concentration,  $C_{s,b}$ .

salt  $C_{salt}^M = 1.328$  M. Also,  $\sigma = 0.025$  corresponds to the area density of surface charge  $\sigma_0 = \sigma(1/a^2) = 10^{-3} e \text{ \AA}^{-2}$ .

First, we determine the above two regimes by varying  $U_0$  from  $-0.5$  to  $0$ . By setting  $U_0 = 0$  in salt-free solution, we can obtain the electrostatic interaction dominated regime. In this case, only electrostatic interaction exists between the cylindric surface and PE monomers. Additionally, there is no screening effect from the salt.

However, the short-range non-Coulombic interaction dominated regime should be determined by investigating the effect of salt concentration on the surface excess and charge inversion ratio for different values of  $U_0$ . This is according to the fact that when the short-range non-Coulombic interaction becomes strong enough to dominate the PE adsorption process, both surface excess and charge inversion will increase as salt concentration increases. Otherwise, they both decrease with increasing salt concentration.

We now begin to establish the short-range non-Coulombic dominated regime. The effect of salt concentration,  $C_{s,b}$ , on the surface excess,  $\Gamma$ , and charge inversion ratio,  $\sigma_{cp}/\sigma$ , has been shown in Figure 1 at  $r_0 = 6 \approx R_g$  for different values of  $U_0$ . For lower chemical attractive potential ( $U_0 = 0, -0.1$ , and  $-0.2$ ),  $\Gamma$  decrease and  $\sigma_{cp}/\sigma$  increase with increasing  $C_{s,b}$ . It is due to the fact that as the lower chemical attractive potential cannot compensate for the entropy loss of PE chains after been adsorbed onto the surface, the adsorption of PE is mainly governed by the surface–PE electrostatic interaction. As a result, increasing salt concentration can weaken PE adsorption by the screening effect from the salt, which results the decreasing of  $\Gamma$  and the increasing of  $\sigma_{cp}/\sigma$ . However, when the chemical attractive potential becomes strong enough, i.e.,  $U_0 = -0.4$  and  $-0.5$ , both  $\Gamma$  and  $\sigma_{cp}/\sigma$  have the reverse behaviors. It is due to the fact that surface–PE electrostatic interaction has few effects on PE adsorption in this case. Additionally, the increasing of salt concentration can also enhance screening the PE monomer–monomer repulsion. Both of them can increase the value of  $\Gamma$ . Thus,  $U_0 = -0.4$  and  $-0.5$

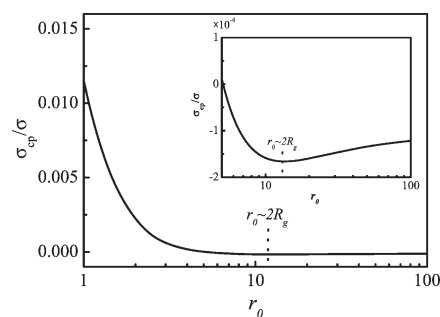


**Figure 2.** Cylindrical radius,  $r_0$ , dependence of the charge inversion ratio,  $\sigma_{cp}/\sigma$ , in the electrostatic interaction dominated regime with bulk concentration of salt  $C_{s,b} = 0$ , surface area charge density  $\sigma = 0.1$ , PE chain charge fraction  $p = 0.5$ , and solvent quality  $\chi_{ps} = 0.1$  for short-range non-Coulombic interaction  $U_0 = 0$ . The insert is the detail for the crossover point of the cylinder radius. Only moderate charge inversion ( $\sigma_{cp}/\sigma \approx -2 \times 10^{-4}$ ) happens in this case.

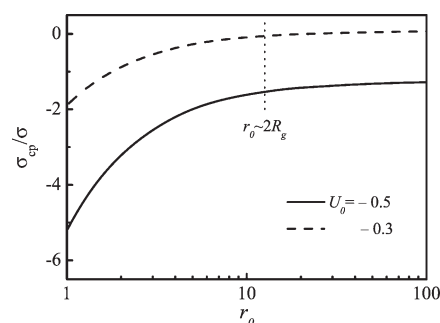


**Figure 3.** Cylindrical radius,  $r_0$ , dependence of the charge inversion ratio,  $\sigma_{cp}/\sigma$ , with bulk concentration of salt  $C_{s,b} = 0.1$ , surface area charge density  $\sigma = 0.025$ , PE chain charge fraction  $p = 0.1$ , and solvent quality  $\chi_{ps} = 0.1$  for the two short-range non-Coulombic interactions  $U_0 = -0.3$  and  $-0.5$ . When  $r_0 < 2R_g$ , charge inversion increases with decreasing  $r_0$ , and strong charge inversion  $\sigma_{cp}/\sigma = -1.9$  and  $-5.2$  have been obtained in large surface curvature ( $r_0 = 1$ ) for  $U_0 = -0.3$  and  $-0.5$ , respectively. As  $r_0 > 2R_g$ ,  $\sigma_{cp}/\sigma$  nearly does not change with  $r_0$ .

correspond to the short-range non-Coulombic dominated regime (the value of  $U_0$  is not universal and will be explained in the end of this section). It is worth to note that in the present weakly charged system whether it being in the electrostatic interaction dominated regime or short-range non-Coulombic interaction dominated regime mainly depends on  $U_0$ . Moreover, Figure 1 shows that full charge inversion usually happens under the conditions of high salt concentration and strong enough surface–PE short-range non-Coulombic interaction. It should be noted that this result is in agreement with other theoretical (in the planar surface system) and experimental results.<sup>7,16,23</sup> Especially, there is a crossover regime around  $U_0 = -0.3$  at which both  $\Gamma$  and  $\sigma_{cp}/\sigma$  nearly do not change with  $C_{s,b}$ .

Figures 2 and 3 show the effects of surface curvature, characterized by cylinder radius  $r_0$ , on the charge inversion ratio  $\sigma_{cp}/\sigma$ . Figure 2 corresponds to the electrostatic interaction dominated regime ( $U_0 = 0$ ,  $C_{s,b} = 0$ ,  $p = 0.5$ ), in which with decreasing the cylinder radius from  $r_0 = 100$  to  $r_0 = 12 \approx 2R_g$ ,  $\sigma_{cp}/\sigma$  decreases very slowly. When the cylinder radius is less than  $2R_g$ , however,  $\sigma_{cp}/\sigma$  increases quickly, and no charge inversion happens in the large surface curvature regime. Moreover, we can only observe moderate charge inversion ( $\sigma_{cp}/\sigma \approx -2 \times 10^{-4}$ ) in this case. However, a different dependence of  $\sigma_{cp}/\sigma$  on  $r_0$  has been found in Figure 3, in which both for the short-range non-Coulombic interaction dominated regime ( $U_0 = -0.5$ ) and the crossover regime ( $U_0 = -0.3$ ), the magnitude of  $\sigma_{cp}/\sigma$  increases with decreasing  $r_0$  at a high salt concentration ( $C_{s,b} = 0.1$ ).



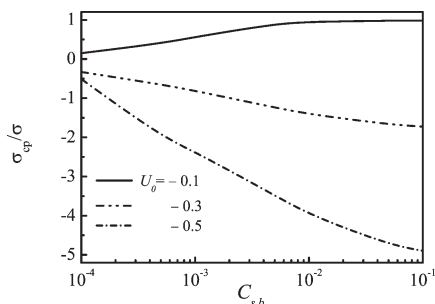


**Figure 4.** Bulk concentration of salt,  $C_{s,b}$ , dependence of the charge inversion ratio,  $\sigma_{cp}/\sigma$ , in large surface curvature (cylindrical radius  $r_0 = 1$ ) for different short-range non-Coulombic interactions  $U_0$  with surface area charge density  $\sigma = 0.025$ , PE chain charge fraction  $p = 0.1$ , and solvent quality  $\chi_{Ps} = 0.1$ . Full charge inversion, for example ( $\sigma_{cp}/\sigma = -1.97$ ), can be obtained at low salt concentration ( $C_{s,b} = 5 \times 10^{-4}$  for  $U_0 = -0.5$ ).

Particularly, large charge inversion ratio  $\sigma_{cp}/\sigma \approx -5.2$  has been observed in the large surface curvature limit ( $r_0 = 1$ ) for  $U_0 = 0.5$ , which indicates that surface curvature does have strong effects on the PE charge inversion phenomena. Also, we can define, approximately, the point of  $r_0 \sim 2R_g$  as a crossover point in these two figures. Note that the crossover point is consistent with our previous work.<sup>25</sup> Actually, another important length scale is the Debye screening length. When Debye length becomes comparable to the length of  $r_0$ , or  $r_0 + d$ , both these lengths will define the region where the curvature effects onto PE adsorption are important. Obviously, the crossover point of  $r_0 \sim 2R_g$  is only reasonable in the systems with short-range non-Coulombic interaction and high salt concentration.

Figure 4 shows the dependence of  $\sigma_{cp}/\sigma$  on  $C_{s,b}$  for three values of  $U_0$  in large surface curvature limit ( $r_0 = 1$ ). For  $U_0 = -0.1$ , no charge inversion happens even at highest salt concentration ( $C_{s,b} = 0.1$ ). For  $U_0 = -0.3$ , full charge inversion happens at higher salt concentration ( $C_{s,b} > 10^{-2}$ ). However, for  $U_0 = -0.5$  full charge inversion ( $\sigma_{cp}/\sigma = -1.973$ ) happens at a low salt concentration ( $C_{s,b} = 5 \times 10^{-4}$ ). This behavior is different from Figure 1b, in which all the parameters are the same as Figure 4 except the surface curvature. This result shows that the effect of surface curvature on charge inversion phenomena is important and leads to the change inversion condition, or strong charge inversion can happen at low salt concentration in large surface curvature limit and with strong short-range interaction. The results also shows that the surface-PE short-range non-Coulombic interaction is the main driving force of charge inversion phenomena.

Now, we study the effect of the area density of surface charge,  $\sigma$ , on charge inversion phenomena in the above two regimes, separately. Figure 5a is in the electrostatic interaction dominated regime with  $U_0 = 0$ ,  $C_{s,b} = 0$ , and  $p = 0.5$ , while Figure 5b is in the non-Coulombic regime with  $U_0 = -0.5$ ,  $C_{s,b} = 0.1$ , and  $p = 0.1$ . Figure 5a shows that  $\sigma_{cp}/\sigma$  decreases as  $\sigma$  increases, and no charge inversion happens. However, Figure 5b shows a different dependence of  $\sigma_{cp}/\sigma$  on  $\sigma$ ; i.e., charge inversion ratio increases as  $\sigma$  decreases. The main reason is as follows: for strong  $U_0$ , the short-range non-Coulombic interaction can dominate the value of  $\Gamma$ , and decreasing  $\sigma$  has few effects on  $\Gamma$ . From the definition of charge inversion ratio  $\sigma_{cp}/\sigma = 1 - p\Gamma/\sigma r_0$ , one can find that  $\sigma_{cp}/\sigma$  decreases, or the charge inversion increases, with decreasing  $\sigma$ . Moreover, we investigate the dependence of  $\sigma_{cp}/\sigma$  on  $\sigma$  in large cylinder radius limit which represents a planar surface. We find strong charge inversion in both of cylindric surface ( $r_0 = 6$ ) and planar surface ( $r_0 = 600$ ).

In order to understand the above strong charge inversion phenomena well, we study the corresponding polymer density

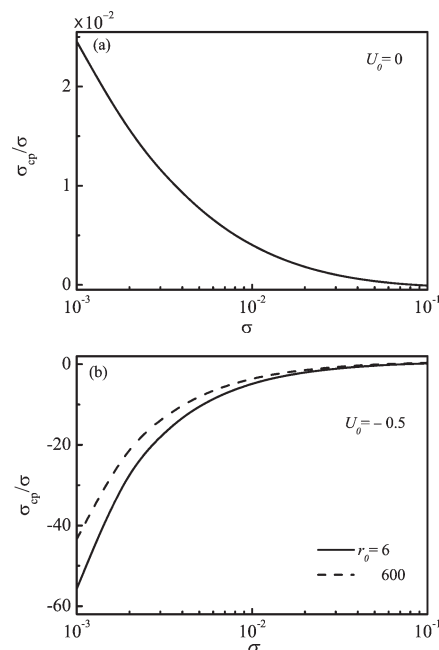


**Figure 5.** Surface area charge density  $\sigma$  dependence of the charge inversion ratio  $\sigma_{cp}/\sigma$ . (a) is in the electrostatic dominated regime with short-range non-Coulombic interaction  $U_0 = 0$ , bulk concentration of salt  $C_{s,b} = 0$ , PE chain charge fraction  $p = 0.5$ , and solvent quality  $\chi_{Ps} = 0.1$  for cylindrical radius  $r_0 = 6$ . (b) is in the short-range dominated regime with  $U_0 = -0.5$ ,  $C_{s,b} = 0.01$ ,  $p = 0.1$ , and  $\chi_{Ps} = 0.1$  for  $r_0 = 6$  and 600.

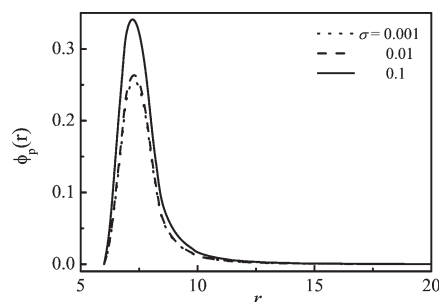


**Figure 6.** Radial monomer volume fraction for cylindrical radius  $r_0 = 6$ , PE chain charge fraction  $p = 0.1$ , bulk concentration of salt  $C_{s,b} = 0.01$ , solvent quality  $\chi_{Ps} = 0.1$ , short-range non-Coulombic interaction  $U_0 = -0.5$ , and surface area charge densities  $\sigma = 0.001$ , 0.01, and 0.1.

profiles near the cylindric surface as shown in Figure 6, which is similarly to the studies for spherical particles in another recent study.<sup>44</sup> From Figure 6 one can find that almost all the PE chains overcompensating adsorbing surface are located within the thickness of the short-range non-Coulombic interaction well. As we take the surface potential range  $d \approx 2$ , the outer boundary of the thickness of  $U_0$  well locates around the point  $r \approx 8$  for  $r_0 \approx 6$ . Furthermore, it is worth to note that due to the strong short-range non-Coulombic interaction, e.g.  $U_0 = -0.5$ , decreasing the surface area charge density  $\sigma$  from 0.1 to 0.001 leads to only small changes of the polymer profiles. Moreover, the surface excess  $\Gamma$  also decreases only a little, e.g.,  $\Gamma = 4.7135$ , 3.5252, and 3.4040, corresponding to  $\sigma = 0.1$ , 0.01, and 0.001, respectively. In the limit of low surface charge densities, according to the definition of charge inversion ratio in eq 10, the second term on the right side dominates charge inversion ratio, and thus we can obtain quite large overcharging. Note that these results in Figures 5 and 6 give further demonstration that it is essential to have an attractive surface in the charge inversion phenomena. The present results

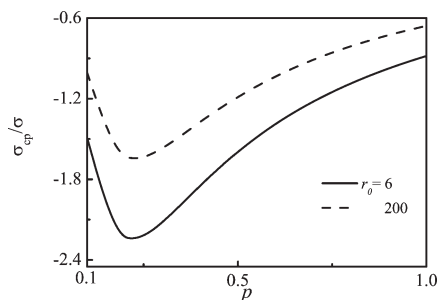


**Figure 7.** PE chain charge fraction  $p$  dependence of the charge inversion ratio  $\sigma_{cp}/\sigma$  for two cylindrical radii  $r_0 = 6$  and 200 with short-range non-Coulombic interaction  $U_0 = -0.5$ , bulk concentration of salt  $C_{s,b} = 0.01$ , surface area charge density  $\sigma = 0.025$ , and solvent quality  $\chi_{Ps} = 0.1$ .

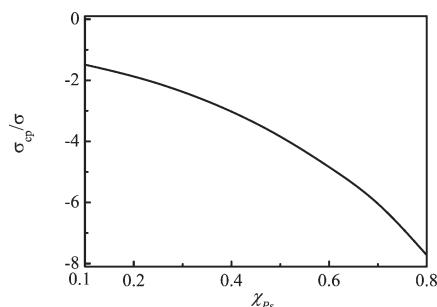


**Figure 8.** Solvent quality  $\chi_{Ps}$  dependence of the charge inversion ratio  $\sigma_{cp}/\sigma$  with short-range non-Coulombic interaction  $U_0 = -0.5$ , bulk concentration of salt  $C_{s,b} = 0.01$ , surface area charge density  $\sigma = 0.025$ , PE chain charge fraction  $p = 0.1$ , and cylindrical radius  $r_0 = 6$ .

well captures the strong charge inversion obtained in other theoretical<sup>23,45</sup> and experimental results.<sup>7</sup> Wang studied planar surfaces adsorbing flexible polyelectrolytes.<sup>23</sup> By varying  $\sigma$  from 0.004 to 0.04 (with  $a = 0.45$  nm), the strong charge inversion on attractive surfaces at high salt concentrations is obtained. Shubin and Linse studied the adsorption of flexible polyacrylamide (CPAM) onto monodisperse silica particles both experimentally and theoretically.<sup>45</sup> They used a charge-regulating surface whose charge density varies with solution pH, salt concentration, and PE concentration. For attractive surfaces and high salt concentrations, they obtained the same dependence tendency of  $\sigma_{cp}/\sigma$  on  $\sigma$  as ours.

Also, we study the effects of the rest two parameters on this phenomena in the regime  $r_0 < 2R_g$ , i.e., the charge fraction of PE chain,  $p$ , and the solvent quality,  $\chi_{Ps}$ . As  $p$  can enhance both surface–PE electrostatic interaction and PE monomer–monomer repulsion, there must be a minimum in  $\sigma_{cp}/\sigma$  as  $p$  varies from 0 to 1. When  $p$  increase first, it can promote the PE adsorption by enhancing surface–PE electrostatic interaction. However, when  $p$  becomes large enough, the monomer–monomer repulsion becomes the main factor and leads to the decreasing of PE adsorption. Numerical result in Figure 7 just verifies this expectation, in which the dependences of  $\sigma_{cp}/\sigma$  on  $p$  both for small cylinder radius  $r_0 = 6$  and large cylinder radius  $r_0 = 200$  at a relatively high salt concentrations ( $C_{s,b} = 0.01$ ) are shown. It is worth noting that the dependence of  $\sigma_{cp}/\sigma$  on  $p$  for  $r_0 = 6$  is very similar as that for  $r_0 = 200$ , which means that  $p$  has almost the same effect on  $\sigma_{cp}/\sigma$  for different surface curvature. Figure 8 shows the effect of  $\chi_{Ps}$  on  $\sigma_{cp}/\sigma$  for  $r_0 = 6$  at  $C_{s,b} = 0.01$ . The charge inversion increases with increasing  $\chi_{Ps}$ , and strong charge inversion  $\sigma_{cp}/\sigma = -7.72$  is obtained at  $\chi_{Ps} = 0.8$ . The reason is that PE chains in poor solvent conditions means that the PE-backbone is hydrophobic, which can create an effective attraction to the surface.<sup>22</sup> Specially, the results in Figures 7 and 8 well

capture the behavior of  $p$  and  $\chi_{Ps}$  on  $\sigma_{cp}/\sigma$ , as in Wang's investigation for the planar surface case.<sup>23</sup>

Finally, we discuss the limitation of the present model. We obtain the short-range non-Coulombic interaction dominated regime by selecting some special values of  $U_0$ . However, the values of  $U_0$  corresponding to this regime are not absolute because they are function of the polymer charge fraction and the area density of surface charge. Thus,  $U_0 = -0.4$  and  $-0.5$  in the present model are not universal corresponding to the short-range non-Coulombic interaction dominated regime but only limit to these weakly charged systems which we choose. Moreover, in the recent study<sup>46</sup> for the spherical surface with a short-range attractive square-well potential, it is shown that the finite extension of the surface potential and the surface curvature have combined effects on the adsorption of polymers. In this paper, we only study the effect of surface curvature on charge inversion phenomena for the fixed value of the potential range,  $d$ . Also, fixing the persistence length of PEs is another limitation of the present model because the persistence length is a function of the salt concentration according to the studies by Dobrynin et al.<sup>5,47</sup> Another approximation is that we use a simple model for the surface–PE short-range non-Coulombic interaction and further assume that it does not change with the cylinder radius. Actually, a changeable short-range interaction is more physical. Furthermore, omitting the volume of the small ions is also a limitation of the present work. These ions compete with polymers for surface adsorption and do affect the PE charge inversion. Finally, we cannot give the exact conformation of PE chains in the adsorbed layers, which is also an interesting topic in polymer science. Extension to consider all the limitations will be presented in future works. However, despite these limitations, we believe that the present model gives an insight for the charge inversion phenomenon in cylindric systems.

#### IV. Conclusions

Within the continuum SCFT including multichain interactions, we study the charge inversion phenomena by flexible polyelectrolytes adsorbed onto charged cylindric surfaces. We mainly focus on the effects of surface curvature on the charge inversion ratio,  $\sigma_{cp}/\sigma$ . The effects of salt concentration,  $C_{s,b}$ , the density of surface charges,  $\sigma$ , the charge fraction of PE chain,  $p$ , and the solvent quality,  $\chi_{Ps}$ , on  $\sigma_{cp}/\sigma$  are also studied. Numerical results show that surface curvature does have strong effect on  $\sigma_{cp}/\sigma$ . Strong charge inversion has been obtained in the large surface curvature limit. In particular, we find that full charge inversion can be obtained even at a low salt concentration with strong enough short-range non-Coulombic interaction in the limit of large surface curvature. Surface curvature and the area density of surface charges have different effects on  $\sigma_{cp}/\sigma$  in the surface–PE electrostatic interaction dominated regime and the surface–PE short-range non-Coulombic interaction dominated regime. As decreasing the cylinder radius and surface charge density,  $\sigma_{cp}/\sigma$  will increase in the first regime while it will decrease in the second regime. We also obtain a crossover point around  $r_0 \sim 2R_g$ . When  $r_0$  goes further than it, the surface curvature will lose its effect on the charge inversion phenomena. Numerical results also show that the effects of  $p$  and  $\chi_{Ps}$  on  $\sigma_{cp}/\sigma$  in the present cylindric systems are the same as those in planar systems. Finally, our results give a further demonstration that the surface–PE short-range non-Coulombic interaction is the main driving force of the charge inversion phenomena, which is in agreement with the other theoretical and experimental results. This simple model gives good insight into the problem of charge inversion and can serve as a starting point for the multilayer formation on cylindric surface.

**Acknowledgment.** We sincerely thank Prof. An-Chang Shi for the helpful discussions. Also, we thank Dr. Shuanhu Qi,

Dr. Xinghua Zhang, and Tongchuan Suo for discussions. This work is supported by the National Natural Science Foundation of China NSFC 20990234, NSFC 20874111, NSFC 50821062, and NSFC 20973176 and also the Grant from Chinese Academy of Sciences KJCX2-YW-206.

## References and Notes

- (1) Fleer, G. J.; Cohen Stuart, M. A.; Scheutjens, J. M. H. M.; Gasev, T.; Vincent, B. *Polymer at Interfaces*; Chapman and Hall: London, 1993.
- (2) Hammond, P. T. *Curr. Opin. Colloid Interface Sci.* **1999**, *4*, 430.
- (3) Grosberg, A. Yu.; Nguyen, T. T.; Shklovskii, I. *Rev. Mod. Phys.* **2002**, *74*, 329.
- (4) Netz, R. R.; Andelman, D. *Phys. Rep.* **2003**, *380*, 1.
- (5) Dobrynin, A. V.; Rubinstein, M. *Prog. Polym. Sci.* **2005**, *30*, 1049.
- (6) Berndt, P.; Kurihara, K.; Kunitake, T. *Langmuir* **1992**, *8*, 2486.
- (7) Shubin, V. J. *Colloid Interface Sci.* **1997**, *191*, 372.
- (8) Berret, J. J. *Chem. Phys.* **2005**, *123*, 164703.
- (9) Decher, G. *Science* **1997**, *277*, 1232.
- (10) Schonhoff, M. *J. Phys.: Condens. Matter* **2003**, *15*, R1781.
- (11) Cho, J.; Quinn, J. F.; Caruso, F. *J. Am. Chem. Soc.* **2004**, *126*, 2270.
- (12) Shiratori, S. S.; Rubner, M. F. *Macromolecules* **2000**, *33*, 4213.
- (13) Tomita, S.; Sato, K.; Anzai, J. *Colloid Interface Sci.* **2008**, *326*, 35.
- (14) Dubas, S. T.; Schlenoff, J. B. *Macromolecules* **1999**, *32*, 8153.
- (15) Voigt, U.; Jaeger, W.; Findenegg, G. H.; Klitzing, R. V. *J. Phys. Chem. B* **2003**, *107*, 5273.
- (16) Shafir, A.; Andelman, D. *Phys. Rev. E* **2004**, *70*, 061804.
- (17) Lyklema, J. *Colloids Surf., A* **2006**, *291*, 3.
- (18) Kotov, N. A. *Nanostruct. Mater.* **1999**, *12*, 789.
- (19) Poptoshev, E.; Schoeler, B.; Caruso, F. *Langmuir* **2004**, *20*, 829.
- (20) Stockton, W. B.; Rubner, M. F. *Macromolecules* **1997**, *30*, 2717.
- (21) Kharlampieva, E.; Sukhishvili, S. A. *Macromolecules* **2003**, *36*, 9950.
- (22) Shafir, A.; Andelman, D. *Eur. Phys. J. E* **2006**, *19*, 155.
- (23) Wang, Q. *Macromolecules* **2005**, *38*, 8911.
- (24) Wang, Q. *J. Phys. Chem. B* **2006**, *110*, 5825.
- (25) Man, X. K.; Yang, S.; Yan, D. D.; Shi, A. C. *Macromolecules* **2008**, *41*, 5451.
- (26) Muthukumar, M. *J. Chem. Phys.* **1987**, *86*, 7230.
- (27) van Goeler, F.; Muthukumar, M. *J. Chem. Phys.* **1994**, *100*, 7796.
- (28) Winkler, R. G.; Cherstvy, A. G. *Phys. Rev. Lett.* **2006**, *96*, 0066103.
- (29) Yingjie, L.; Dubin, P. L.; Spindler, R.; Tomalia, D. A. *Macromolecules* **1995**, *28*, 8426.
- (30) Feng, X. H.; Dubin, P. L.; Zhang, H. W.; Kirton, G. F.; Bahadur, P.; Parotte, J. *Macromolecules* **2001**, *34*, 6373.
- (31) Netz, R. R.; Joanny, J. F. *Macromolecules* **1999**, *32*, 9026.
- (32) Kunze, K. K.; Netz, R. R. *Phys. Rev. Lett.* **2000**, *85*, 4389.
- (33) Kunze, K. K.; Netz, R. R. *Europhys. Lett.* **2002**, *58*, 299.
- (34) Kunze, K. K.; Netz, R. R. *Phys. Rev. E* **2002**, *66*, 011918.
- (35) Gurovitch, E.; Sens, P. *Phys. Rev. Lett.* **1999**, *82*, 339.
- (36) Golestanian, R. *Phys. Rev. Lett.* **1999**, *83*, 2473.
- (37) Shi, A. C.; Noolandi, J. *Macromol. Theory Simul.* **1999**, *8*, 214.
- (38) Wang, Q.; Taniguchi, T.; Fredrickson, G. H. *J. Phys. Chem. B* **2004**, *108*, 6733; **2005**, *109*, 9855.
- (39) Creager, A. N. *The Life of a Virus: Tobacco Mosaic Virus as an Experimental Model, 1930–1965*; University of Chicago Press: Chicago, IL, 2002.
- (40) Rajangam, K.; Behanna, H. A.; Hui, M. J.; Han, X.; Hulvat, J. F.; Lomasney, J. W.; Stupp, S. I. *Nano Lett.* **2006**, *6*, 2086.
- (41) van de Steeg, H. G. M.; Stuart, M. A. C.; de Keizer, A.; Bijsterbosch, B. H. *Langmuir* **1992**, *8*, 2538.
- (42) Yang, S.; Yan, D. D.; Shi, A. C. *Macromolecules* **2006**, *39*, 4168.
- (43) Press, W. H.; Teukolsky, S. A.; Vetterling, W. T.; Flannery, B. P. *Numerical Recipes in C: the Art of Scientific Computing*, 2nd ed.; Cambridge University Press: Cambridge, UK, 2002; Chapter 9.7.
- (44) Winkler, R. G.; Cherstvy, A. G. *J. Phys. Chem. B* **2007**, *111*, 8486.
- (45) Shubin, V.; Linse, P. *Macromolecules* **1997**, *30*, 5944.
- (46) Chervanyov, A. I.; Heinrich, G. *J. Chem. Phys.* **2009**, *131*, 104905.
- (47) Dobrynin, A. V.; Colby, R. H.; Rubinstein, M. *Macromolecules* **1995**, *28*, 1859.